Proceedings of the Combustion Institute, Volume 28, 2000/pp. 911–917

CONVECTIVE BURNING IN GAPS OF PBX 9501

H. L. BERGHOUT, S. F. SON AND B. W. ASAY
Los Alamos National Laboratory
Los Alamos, NM 87545, USA

Impact or thermal ignition of high explosives results in deformation that can lead to fracture. Fracture, combined with high pressure, dramatically increases the available surface area and potentially changes the mode of combustion. Recent impact and cook-off experiments on PBX 9501 (HMX, octahydro-1,3,5,7-tetranitro-1,3,5,7-tetrazocine, with a binder) have shown complex cracking patterns caused by impact or pressurization. Fast reactive waves have been observed to propagate through the cracks at about 500 m/s. We present experiments that investigate the propagation of fast reactive waves in cracks of PBX 9501, focusing on the reactive wave velocity and on the interplay of pressure and crack size. Experiments at initial pressures of 6.0 MPa reveal monotonic reactive wave propagation velocities of around 7 m/s for a 100 μm slot. We observe reactive wave velocities as high as 100 m/s in experiments at initial pressures of 17.2 MPa and various slot widths. Similar experiments at lower pressure exhibit oscillatory reactive wave propagation in the slot with periodic oscillations whose frequencies vary with combustion vessel pressure. This is the first reported observation of oscillatory combustion in cracks of an energetic material such as PBX 9501. Threshold pressure experiments for combustion propagation into closed-end slots of PBX 9501 find that combustion propagates into 2 mm, 1 mm, 100 μm, 50 μm, and 25 μm slots at approximately 0.1, 0.2, 0.9, 1.6, and 1.8 MPa, respectively.

Introduction

The shift from conductive or normal burning to convective burning is an important step of the deflagration-to-detonation transition in explosives and other energetic materials [1–3]. Conductive burning involves primarily conductive heat transfer from the gas-phase flame region to the surface and, to a lesser extent, radiation transport from the gas to the solid. In contrast, convective burning involves heat transfer augmented by mass flow. Defects increase the available surface area where combustion can occur and greatly increase the likelihood of convective burning in energetic materials. The effect of defects on combustion has major implications for the safety and reliability of energetic materials.

Voids and cracks in explosives may result from numerous environmental and physical factors. Impact, aging, and variations in temperature and pressure associated with combustion are a few of the factors that can produce defects. At sufficiently high pressures, the surface area of a defect becomes accessible to deflagration. Defects can trap the hot reaction products, creating the necessary pressure gradient for convective burning. Numerous studies exist on the effects of voids and cracks on the combustion of some common propellants [3,4], but there are relatively few studies of the effects of voids and cracks on the combustion of high explosives [3]. Ramaswamy and Field have studied hot spot and crack propagation in single crystals of RDX [5]. Explosives such as HMX (octahydro-1,3,5,7-tetranitro-1,3,5,7-tetrazocine) typically use a binder that makes it possible to shape the explosive. Binder affects the number, shape, and size of voids and influences somewhat the kinetics of combustion [6]. Our studies investigate the effects of voids and cracks on the combustion of PBX 9501, HMX with an estane-based binder. In addition to improving our understanding of the safety aspects related to PBX 9501, these experiments provide useful data for current efforts to develop models of violent, explosive reactions.

Recent experiments highlight the importance of cracks and voids in the ignition, combustion, and reaction violence of PBX 9501. Fig. 1 shows a PBX 9501 target from a modified Steven Test conducted by Idar et al. [7]. The Steven Test measures the sensitivity of an energetic material to the low-speed impact of a blunt, mild steel projectile. Its results are used to postulate a damage sequence that leads to ignition. Radial cracks emanating from the impact point are apparent in Fig. 1 for a test in which no sustained reaction occurred. Idar et al. found that damaged PBX 9501 has a significantly lower impact threshold for violent reaction than does pristine material.

Henson et al. conducted shear impact experiments using thin disks of PBX 9501 [8]. They drove a rectangular steel plunger into the lightly confined disk at about 100 m/s. Plunger impact causes both shear and non-shear fracturing, with reaction initiated

Report Documentation Page

Form Approved
OMB No. 0704-0188

1. REPORT DATE	2. REPORT TYPE	3. DATES COVERED
04 AUG 2000	**N/A**	**-**

4. TITLE AND SUBTITLE	5a. CONTRACT NUMBER
Convective Burning in Gaps of PBX 9501	5b. GRANT NUMBER
	5c. PROGRAM ELEMENT NUMBER
6. AUTHOR(S)	5d. PROJECT NUMBER
	5e. TASK NUMBER
	5f. WORK UNIT NUMBER
7. PERFORMING ORGANIZATION NAME(S) AND ADDRESS(ES) **Los Alamos National Laboratory Los Alamos, NM 87545, USA**	8. PERFORMING ORGANIZATION REPORT NUMBER
9. SPONSORING/MONITORING AGENCY NAME(S) AND ADDRESS(ES)	10. SPONSOR/MONITOR'S ACRONYM(S)
	11. SPONSOR/MONITOR'S REPORT NUMBER(S)

12. DISTRIBUTION/AVAILABILITY STATEMENT
Approved for public release, distribution unlimited

13. SUPPLEMENTARY NOTES
See also ADM001790, Proceedings of the Combustion Institute, Volume 28. Held in Edinburgh, Scotland on 30 July-4 August 2000.

14. ABSTRACT

15. SUBJECT TERMS

16. SECURITY CLASSIFICATION OF:			17. LIMITATION OF ABSTRACT	18. NUMBER OF PAGES	19a. NAME OF RESPONSIBLE PERSON
a. REPORT	b. ABSTRACT	c. THIS PAGE			
unclassified	**unclassified**	**unclassified**	**UU**	**7**	

Standard Form 298 (Rev. 8-98)
Prescribed by ANSI Std Z39-18

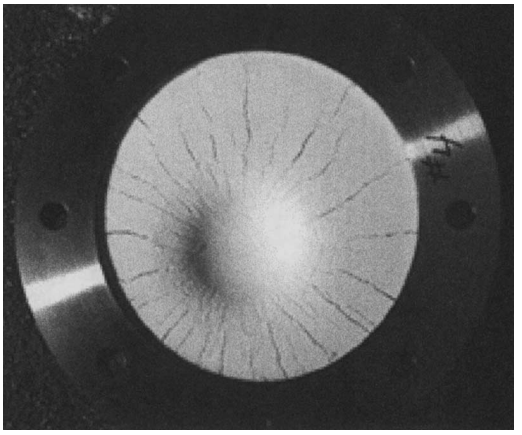

FIG. 1. PBX 9501 target showing the extensive radial cracking around the impact point that results from low-speed impact by a blunt projectile, from Idar et al. [7].

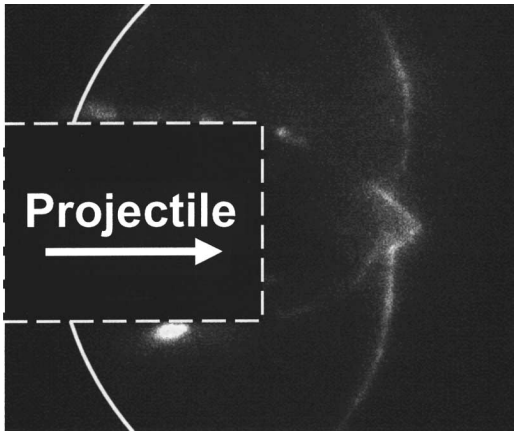

FIG. 2. Ignition of PBX 9501 initiated by shearing-projectile impact, from Henson et al. [8]. The solid curved line approximately outlines the disk of PBX 9501, while the dashed box outlines the projectile that has impacted the disk from the left. Luminous reaction is seen along the edge of the projectile, in the shear cone in front of the projectile, and in other stress cracks caused by the impact.

along fracture zones as shown in Fig. 2. Skidmore et al., at Los Alamos National Laboratory, used visible microscopy to study damaged samples recovered from the shear impact experiments and found that the HMX along the fracture zones showed clear signs of heating and reaction [9].

Evidence of the importance of combustion in cracks also appears in elevated-temperature experiments, such as mechanically coupled cook-off (MCCO). Dickson et al. slowly heated a confined sample of PBX 9501 to a well-defined temperature,

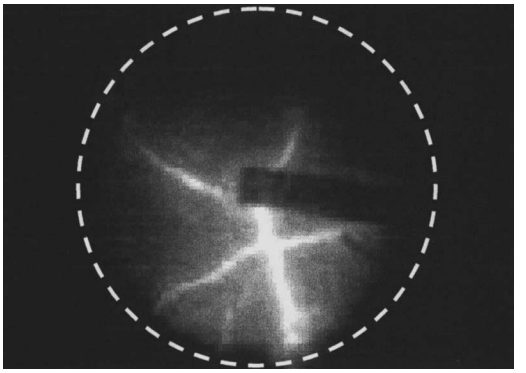

FIG. 3. Luminous reaction in cracks of PBX 9501 during mechanically coupled cook-off experiment, from Dickson et al. [10]. The dashed line approximately outlines the disk of PBX 9501. The dark rectangular area intruding from the right is a foil sheet used for sample ignition. Ignition of a hole at the center of the sample with a hot NiCr wire pressurizes the sample, causing cracking, and luminous reaction can be seen in these cracks.

then ignited the sample. They detected reaction, indicated by luminous emission, throughout intricate networks of cracks that are caused by pressurization due to production of reactive gases [10]. Fig. 3 shows luminous reaction in cracks during an MCCO experiment. The fast reactive waves, indicated by the luminosity, propagate through the cracks at velocities on the order of 500 m/s.

Maienschein and Chandler reported erratic burn rates in HMX-based explosives with low binder content (~5 wt %) but observed no such erratic rapid burn rates for similar explosives with greater binder content (~15 wt %) [11]. Similar experiments by Son et al. visually observed erratic burn rates in high-nitrogen compounds; video records verified that erratic burn rates resulted from reaction propagating into very small cracks that were present in the sample [12]. This observation is consistent with the Maienschein and Chandler experiment, in which smaller amounts of binder made defects and voids more likely, leading to the reported erratic burn rates.

Experimental Setup

Figure 4 is an example of the sample configuration for the results reported in this study. Two pieces of PBX 9501 compose the sample. One of the pieces is machined so that when combined with the second piece, the two pieces form an assembly with a flat slot of the desired width in the middle. Our lower-pressure experiments use sample halves with dimensions of 15.0 × 7.5 × 40.0 mm, for combined dimensions of 15 × 15 × 40 mm with a flat slot 34.0

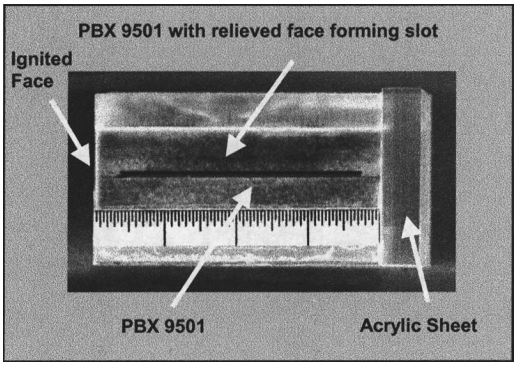

FIG. 4. Example of the lower-pressure sample configuration with a 1 mm slot. Two pieces of PBX 9501 comprise the sample, one of which is relieved in the center (top in this view), so that when the two are combined they form an assembly with well-defined slot dimensions. The high explosive is surrounded on five sides with clear acrylic to inhibit burning. A hot NiCr wire ignites the open sample face.

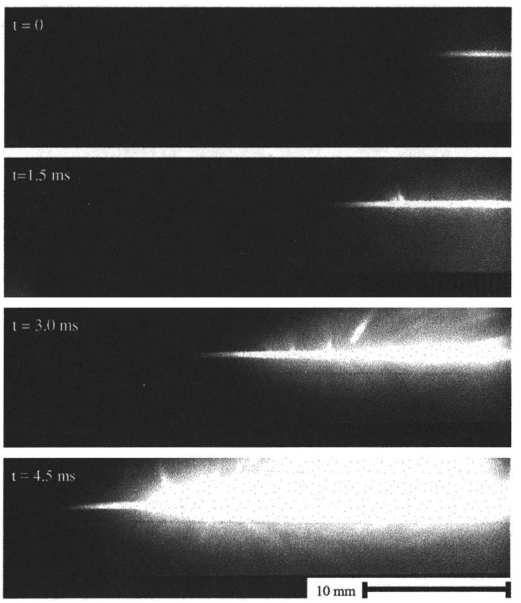

FIG. 5. Sequence of high-speed video images showing the progress of the luminous front into a 100 μm slot during deflagration of a sample of PBX 9501 at an initial pressure of 6.0 MPa. The slot can be seen lying horizontally through the middle of each frame with explosive flats above and below it.

mm in length and of the desired width and 3.0 mm of material at each end. Higher-pressure experiment samples are similar but use less material. Individual halves are 10.0 × 2.0 × 40.0 mm, for combined dimensions of 10.0 × 4.0 × 40.0 mm with a 34.0 mm long slot of the desired width and 3.0 mm of material at each end. Reducing the amount of PBX 9501 in the higher-pressure experiments allows tests with higher initial pressures of Ar without exceeding the maximum designed pressure of the combustion vessel during the experiment. Cell design revisions also provide access for pressure measurements in the slot during the experiment. Resistance-heated NiCr wire ignites one of the faces, and clear 6.35 mm thick acrylic sheets on the remaining five faces inhibit burning along the sides while allowing visual imaging of the slot.

Lower-pressure experiments use initial pressures of Ar up to 6.0 MPa, while higher-pressure experiments use initial pressures from 3.4 to 17.2 MPa. Sample cells are mounted inside a stainless steel pressurized combustion vessel with an internal volume of 2 L and four optical access ports for all experiments at elevated pressures. All experiments are conducted with the pressure vessel and sample initially at room temperature, ~293 K.

We use several diagnostic tools to monitor the progression of reactions in the slot. A Canon XL-1 digital video system records the entire event at 30 fps. During the course of the experiments, various high-speed digital imaging systems provided visual information about the progress of the combustion in the slot. Two or three imaging systems were commonly used simultaneously, providing views of the slot from both edges. Olympus Encore MAC-4000S, Kodak EKTAPRO HG 2000, Motion Corder SR-500, and EKTAPRO Model 1000 HR systems at maximum frame rates of 4000, 2000, 500, and 1000 fps, respectively, provide images for the lower-speed experiments. A Red Lake MotionScope PCI 8000S, with frame rates up to 8000 fps, and a Kodak EKTAPRO HS Model 4540, with frame rates up to 40,500 fps, were used for the highest-pressure experiments, in which we observed flame propagation velocities up to 100 m/s.

An Omega Model PX605-10KGI pressure transducer monitors the pressure in the combustion vessel. Additionally, the higher-pressure experiments use PCB Piezotronics Model 113A23 pressure sensors to monitor the transient combustion vessel pressure and the pressure of the slot relative to the combustion vessel. Tektronix Model TDS 460A and TDS 540A digital oscilloscopes capture the pressure sensor outputs for later storage and analysis. Ionization pins inserted into the PBX 9501 slot provide a trigger signal for the video- and pressure-recording systems.

Results and Discussion

Figure 5 displays a sequence of high-speed video images taken with the Kodak EKTAPRO HG 2000

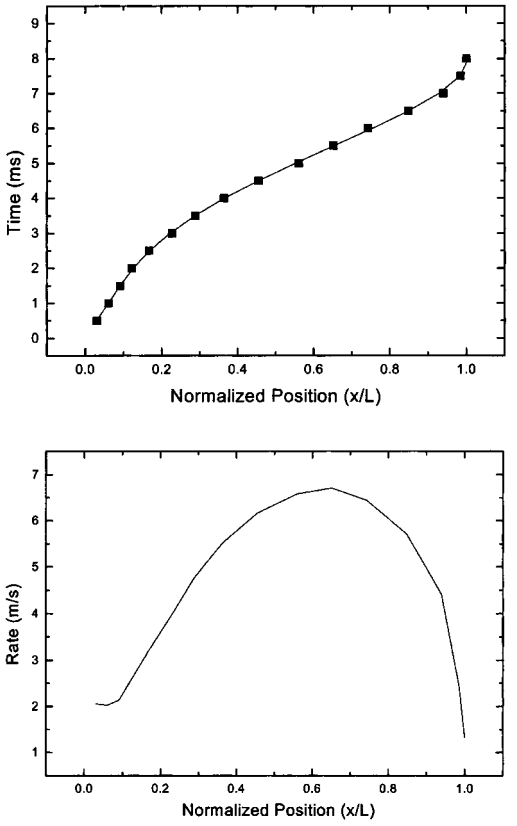

FIG. 6. Plots of time and rate versus normalized position for the progress of the luminous front into a 100 μm slot during deflagration of a sample of PBX 9501 at an initial pressure of 6.0 MPa.

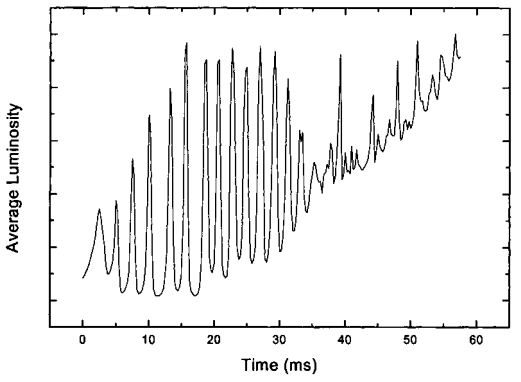

FIG. 7. Plot of the video frame average luminosity versus time for 100 μm slot in PBX 9501 at an initial pressure of 1.4 MPa. Frame luminosity measurements provide information about the oscillatory reaction progress in the slot at both short and long times.

at 2000 fps. These images show the progress of the luminous front into a 100 μm slot in PBX 9501 at an initial pressure of 6.0 MPa, typical of our lower-pressure experiments. Luminous reaction enters the slot on the right and propagates to the left in these views. The relative timing of each of the frames appears as an inset. Exposure is set to capture the leading edge of the luminous reaction front. Consequently, fully ignited regions of the crack are overexposed and video blooming occurs (the crack did not widen significantly at these early times despite the apparent widening caused by the blooming). During the course of the experiment the combustion vessel pressure, as indicated by the Omega pressure gauge, rises gradually to about 6.5 MPa while the first 3 mm of material is consumed and the slot is exposed. Video images capture the progress of the flame into the exposed slot. During the very brief period when the flame spreads into the slot, the combustion vessel pressure is approximately constant but rises rapidly after the slot is fully ignited.

Figure 6 contains plots of time and rate versus normalized position of the luminous flame tip for the sequence of frames in Fig. 5. These plots illustrate the progress of the flame as it propagates into the slot. We determine the progress of the flame by visually monitoring the progress of the luminous tip. The upper plot shows the data with a fourth-degree polynomial fit, indicated by the line. An analytical derivative of the fit, shown in the lower plot, provides a measure of the flame propagation rate. On entering the slot, the flame accelerates and reaches its maximum propagation rate of about 7 m/s two-thirds of the way into the slot. The flame tip then decelerates as it approaches the closed end of the slot. Luminous flame acceleration and deceleration are similar to the behavior Kumar et al. observed in manufactured slots of various composite propellants with an ammonium perchlorate (AP) base [13]. While the behavior of the flame in the slot is similar to that observed by Kumar et al., our experiments differ significantly from theirs. Flame propagation in our experiments is driven entirely by combustion within the slot, while in their experiments Kumar et al. observe the ignition of the slot by externally generated hot gases that are forced into the slot.

At lower initial pressures of 1.4 and 3.4 MPa, the 100 μm slot experiments also reveal initial flame propagation velocities in the 5–10 m/s range, but unlike the 6.0 MPa experiment, they exhibit oscillatory flame propagation and reaction in the slot. Oscillatory behavior, as indicated by integrated luminosity, is apparent even after the luminous flame stops moving in and out of the slot. Fig. 7 plots the average frame luminosity versus time for the 1.4 MPa, 100 μm slot experiment. An Olympus Encore MAC-4000S system operating at 4000 fps recorded the event. The average frame luminosity tracks the intensity of the light emitted from the crack. Frame

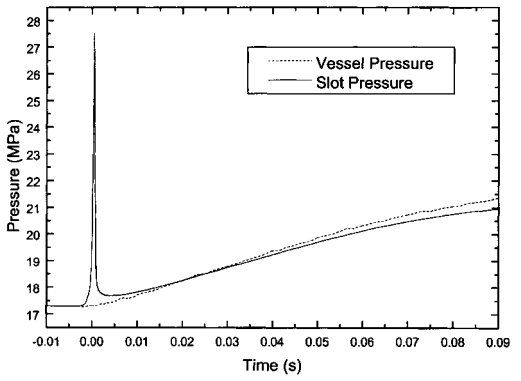

FIG. 8. A typical pressure versus time plot showing the combustion vessel pressure and slot pressure for a 17.2 MPa experiment with a 50 μm slot sample. The spike in the slot pressure trace corresponds to the appearance of luminous reaction in the slot.

luminosity is a useful qualitative measurement of the extent of reaction in the slot, both at early times while the luminous front moves in and out of the slot and at later times when the slot is continually illuminated but the intensity of the light continues to fluctuate. Reaction in the slot fluctuates periodically with a frequency of 400–500 Hz for the 1.4 MPa experiment and 800–900 Hz for the 3.4 MPa experiment. Periodic flashing gradually gives way to steady burning in the slot as the pressure in the combustion vessel rises. The observed low-frequency instabilities are an order of magnitude slower than would be expected from acoustically driven process and are probably similar in origin to the L^* instability common in small rocket motors [14]. L^* instabilities arise from coupling the energetic material's burn rate to bulk pressure and are most common in configurations with a small value of the ratio L^* (combustor cavity volume/nozzle throat area). L^* instabilities are most pronounced in materials whose burn rates are very pressure dependent, such as PBX 9501, which has a conductive burn rate pressure exponent of 0.92 [12]. Bradley and Boggs suggest that convective combustion instabilities could be important in the deflagration-to-detonation transition [3].

A cell revision using less PBX 9501 facilitated experiments at initial pressures up to 17.2 MPa while providing for PCB Piezotronics Model 113A23 pressure transducers to monitor the pressure in the slot. In addition to allowing higher initial pressures, the redesigned cell improved the sample confinement, allowing pressures in the slot to reach higher values than were possible in the original design. Consequently, we have been able to observe much higher reactive wave velocities. Fig. 8 shows pressure versus time traces for an experiment with a 50 μm slot at an initial pressure of 17.2 MPa. The dashed line in Fig. 8 shows the output of the PCB pressure transducer monitoring the vessel pressure. Vessel pressure rises smoothly beginning with sample ignition due to reaction product and heat generation. The solid line in Fig. 8 shows the output of another PCB pressure transducer monitoring the pressure in the slot. Vacuum grease in the pressure transducer port limits the ports' contribution to the slot volume while allowing the pressure transducer to monitor the slot pressure. Initial slot-pressure spikes correspond temporally to the appearance of a fast luminous reactive wave in the slot. Recovered samples reveal that the acrylic sheet surrounding the PBX 9501 cracks during the pressure spike, resulting in a loss of confinement and the subsequent rapid pressure drop. Similar features are common in all of our 100, 50, and 25 μm slot experiments at initial pressures between 3.4 and 17.2 MPa. We observe reactive wave velocities as high as 100 m/s and pressurization rates as high as 15 GPa/s for all of these slot widths and initial pressures. No clear trend associates flame propagation speed with the initial pressure. This is most likely because the flame propagation speed depends more on the pressure differential in the slot than on the vessel pressure under our experimental conditions. Therefore, the strength of the confinement dictates the observed flame propagation speeds. Kumar et al. observed ignition-front propagation velocities near 800 m/s in manufactured slots of several AP-based propellants [13]. Kumar et al. worked at even higher pressurization rates than we have achieved and found that higher pressurization rates produce faster propagation velocities. In addition to the experimental differences, AP-based propellants have a much smaller reaction zone than HMX, which may also play a role in the ignition velocities that are attainable for a give pressurization rate. Our experiment's slot pressures and pressurization rates are limited by the strength of our sample cells. We are currently pursuing higher-pressurization-rate experiments to determine the dependence of the reactive wave velocity on the slot width and initial gas pressure using hardened steel to encase the PBX 9501 sample.

As noted above, high pressure in the slot cracked the acrylic casing, even at the moderate pressures experienced during these experiments. The acrylic casing is much stronger than the PBX 9501 sample. This has significant ramifications for reaction violence and safety in PBX 9501. The rapid pressurization of a sample of PBX 9501 is likely to cause significant fracture, providing new surface area for reaction and leading to an even faster pressurization rate. This sequence of events could run away, drastically increasing reaction violence.

In addition to observing the velocity of the reactive wave as it penetrates the crack, we have carried out experiments to determine the critical pressure for flame propagation into PBX 9501 slots of various

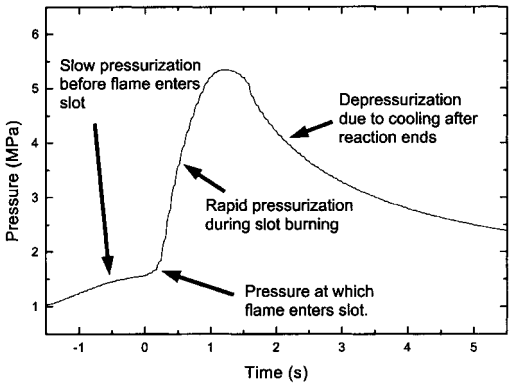

FIG. 9. A typical pressure versus time plot of combustion vessel pressure during a critical pressure experiment. The initial pressure slope is due to deflagration of the ignited face before the flame enters the slot. The pressurization rate increases dramatically when the pressure in the vessel reaches the critical pressure necessary for the flame to enter and consume the slot. We take the pressure at the point where the pressure begins to increase rapidly as the critical pressure.

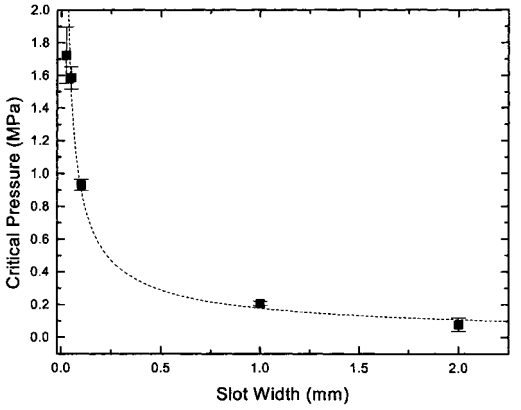

FIG. 10. A plot of critical pressure versus slot width for PBX 9501.

widths. We begin the experiment with the combustion vessel pressurized below the critical pressure for the slot dimension of interest. As the sample burns, the reaction products pressurize the combustion vessel slowly until the critical pressure is reached, at which time the flame enters the slot. Fig. 9 displays a typical pressurization curve of the pressure vessel as measured by the Omega pressure transducer in our critical pressure experiments. Visible imaging verifies that the sharp rise in the combustion vessel pressurization rate corresponds to the flame entering the slot, so we take the pressure at this point to be the critical pressure for burning in the slot.

Combustion propagates into 2 mm, 1 mm, 100 μm, 50 μm, and 25 μm slots at approximately 0.1, 0.2, 0.9, 1.6, and 1.8 MPa, respectively. The observed values are consistent with a simplified theoretical expression for a closed-end slot [3]

$$p_*^{1+2n}\, w^2 = \text{constant} \qquad (1)$$

where p_* is the critical pressure, n is the conductive burn rate pressure exponent, and w is the critical slot width. The dashed line in Fig. 10 results from equation 1, where we have assumed n to equal 0.92, the value for PBX 9501 [12], and fit the constant, which equals 8×10^8 (mks units).

Conclusions

We have observed combustion wave propagation in well-characterized slots of PBX 9501, focusing on the interplay of pressure and slot width on the reaction wave velocity. At an initial pressure of 6.0 MPa, we observed non-oscillatory reactive wave propagation velocities of about 7 m/s in a 100 μm closed end slot and reactive wave velocities as high as 100 m/s in experiments at initial pressures of 17.2 MPa and 25, 50, and 100 μm slot widths. The same experiments, conducted at lower initial pressures, reveal unstable reactive wave propagation in the slot with periodic oscillations that are likely to be related to the L^* instability, common in small rocket engines. We have also investigated the threshold pressure for combustion propagation into slots of PBX 9501. Combustion propagates into 2 mm, 1 mm, 100 μm, 50 μm, and 25 μm slots at approximately 0.1, 0.2, 0.9, 1.6, and 1.8 MPa, respectively.

Acknowledgments

We acknowledge the assistance of C. A. Bolme and D. Rodda with many of the experiments and analysis described here. We acknowledge the support of Los Alamos National Laboratory, under contract W-7405-ENG-36. In particular, we acknowledge the support of the Laboratory Directed Research and Development Program of Los Alamos National Laboratory.

REFERENCES

1. Asay, B. W., Son, S. F., and Bdzil, J. B., *Int. J. Multiphase Flow* 22:923–952 (1996).
2. Belyaev, A. F., and Bobolev, V. K., *Transition from Deflagration to Detonation in Condensed Phases,* National Technical Information Service, Springfield, VA, 1973, 1975 translation ed.
3. Bradley, H. H., and Boggs, T. L., *Convective Burning in Propellant Defects: A Literature Review,* report NWC-TP-6007, Naval Weapons Center, China Lake, CA, 1978.

4. Kumar, M., and Kuo, K. K., in *Fundamentals of Solid Propellant Combustion, Vol. 90,* (K. Kuo and M. Summerfield, eds.) AIAA, New York, 1984, pp. 339–350.
5. Ramaswamy, A. L., and Field, J. E., *J. Appl. Physics* 79:3842–3847 (1996).
6. S. F. Son, H. L. Berghout, C. A. Bolme et al., *Proc. Combust. Inst.* 28:919–924.
7. Idar, D. J., Straight, J. W., Osborn, M. A., et al., in *Shock Compression of Condensed Matter—1999, AIP Conference Proceedings, Vol. 505* (M. Furnish, L. Chhabildas, and R. Hixson, eds.), American Institute of Physics, Melville, NY, 2000, pp. 655–658.
8. Henson, B. F., Asay, B. W., Dickson, P. M., et al., in *Eleventh International Detonation Symposium* (J. Short, ed.), Naval Research Laboratory, Arlington, VA, 2000.
9. Skidmore, C. B., Phillips, D. S., Asay, B. W., et al., in *Shock Compression of Condensed Matter—1999,* AIP Conference Proceedings, Vol. 505, (M. Furnish, L. Chhabildas, and R. Hixon, eds.), American Institute of Physics, Melville, NY, 2000.
10. Dickson, P. M., Asay, B. W., Henson, B. F., et al., in *Eleventh International Detonation Symposium* (J. Short, ed.), Naval Research Laboratory, Arlington, VA, 2000.
11. Maienschein, J. L., and Chandler, J. B., in *Eleventh International Detonation Symposium* (J. Short, ed.), Naval Research Laboratory, Arlington, VA, 2000.
12. Son, S. F., Berghout, H. L., Bolme, C. A., et al., *1999 JANNAF Eighteenth PSHS Meeting, Vol. 1,* CPIA, Columbia, MD, 1999, pp. 101–111.
13. Kumar, M., Kovacic, S. M., and Kuo, K. K., *AIAA J.* 19:610–618 (1981).
14. Price, E. W., in *Nonsteady Burning and Combustion Stability of Solid Propellants, Vol. 143,* (L. De Luca, E. W. Price, and M. Summerfield, eds.) AIAA, New York, 1992, pp. 325–361.